Third-order optical nonlinearities in semiconductor microstructures

L. Banyai
Institut für Theoretische Physik, Universität Frankfurt, D-6000 Frankfurt, Federal Republic of Germany

Y. Z. Hu
Optical Sciences Center, University of Arizona, Tucson, Arizona 85721

M. Lindberg
Department of Physics, University of Arizona, Tucson, Arizona 85721

S. W. Koch
Optical Sciences Center, University of Arizona, Tucson, Arizona 85721
and Department of Physics, University of Arizona, Tucson, Arizona 85721
(Received 29 February 1988)

Optical nonlinearities in semiconductor microcrystallites are analyzed theoretically. The third-order optical susceptibility is evaluated for different crystallite-size regimes ranging from weak quantum confinement, where only the center-of-mass motion of the electron-hole pairs is modified, all the way down to very small quantum dots, where the individual motion of the electrons and holes is confined and the Coulomb attraction is unimportant. Large optical nonlinearities are computed for sufficiently narrow linewidths of the microcrystallites. It is predicted that the induced two-photon absorption resonance (biexciton resonance) shifts from below to above the exciton resonance when the crystallite radius is reduced from bulk to less than the exciton Bohr radius. The magnitude of the expected optical nonlinearities in the different confinement regimes is analyzed for various semiconductor materials.

I. INTRODUCTION

Quantum confinement effects in optically excited semiconductor microstructures arise if at least one spatial dimension of the material becomes comparable to or smaller than the characteristic length scale of an electron-hole pair. Well-known examples of such semiconductor systems are the multiple-quantum-well structures made of alternating layers of active and transparent material. Laser excitation in the appropriate frequency regime generates electron-hole pairs within the quasi-two-dimensional active layers. These layers provide confinement in one space dimension, which is already sufficient to largely enhance in particular excitonic effects.

In two dimensions, the binding energy of the excitons with principal quantum number n is given by[1] $E_n = E_R/(n+\frac{1}{2})^2$, $n=0,1,2,\ldots$, where E_R is the exciton Rydberg, whereas in three dimensions $E_n = E_R/n^2$, $n=1,2,\ldots$. The binding energy of the lowest exciton state is therefore 4 times larger in two than in three dimensions. This particular feature makes exciton effects easily observable even at room temperature, as was shown, e.g., in GaAs-$Al_xGa_{1-x}As$ multiple-quantum-well structures.[2] For more details and for a recent review of the linear and nonlinear optical properties of multiple-quantum-well structures see, e.g., Ref. 3.

Stimulated by the large optical nonlinearities observed in quantum wells, quite recently semiconductor microcrystallites are being investigated, which confine the laser-excited electron-hole pairs in all three space dimensions.[4-15] Presently available examples of such systems are colloids or semiconductor microcrystallite-doped glasses,[4-12] as well as microstructures obtained by sophisticated etching procedures.[13-15] It has been shown that special glasses doped with CdS, CdSe, CuCl, or CuBr crystallites[4] can be fabricated, which clearly exhibit quantum confinement. The microcrystallites in these glasses form out of the supersaturated solid solution of the basic constituents originally brought into the glass melt. The average size of the crystallites follows a universal growth law[4,16] $R \simeq t^{1/3}$, where t is the duration of the heat treatment during which the crystallites actually grow. The crystallite sizes are distributed according to the universal Lifshitz-Slyozov distribution,[16] and they are more or less randomly arranged in the glass matrix. Well controlled average crystallite sizes from around 10 Å up to several 100 Å have been reported in Ref. 4.

The first attempts of manufacturing GaAs microcrystallites have recently been reported.[13-15] Applying an anisotropic reactive ion-etching and/or sophisticated doping procedures to multiple-quantum-well structures, both quantum wires as well as arrays of quantum dots have been fabricated. The luminescence properties of the samples have been investigated, but no detailed studies of the nonlinear optical properties of these systems have been reported yet.

The first theoretical investigations of quantum confinement in semiconductor microcrystallites have been reported by Efros and Efros[4] and by Brus.[5] Various

regimes of quantum confinement have been introduced, depending on the ratio of the crystallite radius R to the Bohr radius of the electron-hole pairs, $a_B=\hbar^2\epsilon_2/\mu e^2$, holes, $a_h=\hbar^2\epsilon_2/m_h e^2$, and electrons, $a_e=\hbar^2\epsilon_2/m_e e^2$, respectively, where $1/\mu=1/m_e+1/m_h$ and ϵ_2 is the background dielectric constant of the semiconductor material. Efros and Efros attributed to these regimes quantization of the exciton, $R>a_B$, quantization of the electron, $a_e>R>a_h$, and quantization of electron and hole, $a_e,a_h>R$, respectively. Using the effective mass approximation these authors showed that the increasing kinetic energy of the confined quasiparticles leads to a blue shift of the electron-hole-pair groundstate energy. This blue shift is always proportional to $1/R^2$, but the prefactors are different in the different confinement regimes.

Optical nonlinearities in various quantum-confinement regimes have been discussed in Refs. 17–20. For crystallite sizes well exceeding the bulk exciton diameter, we have predicted an excitation-induced blue shift of the exciton resonance as a consequence of the plasma screening of the attractive Coulomb interaction between electrons and holes.[17] Large optical nonlinearities for weak quantum confinement have also been predicted by Hanamura,[18] whereas the regime of extremely strong quantum confinement has been discussed in Ref. 19.

In the present paper we calculate the third-order optical nonlinearity in the different size regimes, and we compare the predicted effects with known results both of bulk semiconductors and of atomic systems. In Sec. II we outline the theory of the third-order optical susceptibility and we derive the expression for χ_3. The parameters in χ_3 depend on the confining geometry and are evaluated for the so-called boson model in Sec. III, where this model is generalized to include the effects of weak quantum confinement. In Sec. IV we treat the situation of moderate quantum confinement, where the crystallite radius exceeds the Bohr radius of the hole, but is considerably smaller than the electron Bohr radius. This situation is very interesting for most direct-gap semiconductors due to the large difference of the effective masses of electrons and holes. Our theory predicts that the induced two-photon (biexciton) resonance is shifted from energetically below the exciton resonance in bulk materials to above the exciton resonance under moderate confinement.

In the regime of strong quantum confinement, one may neglect the Coulomb energy in comparison to the confinement energy.[4] Hence, the system becomes an equivalent to an atomic system with discrete levels. For completeness, we compute the third-order susceptibility also for these conditions in Sec. V. The results for the different regimes of quantum confinement are summarized in Sec. VI and the magnitude of the expected nonlinearities is evaluated for a variety of semiconductor materials.

II. THEORY OF THE NONLINEAR OPTICAL SUSCEPTIBILITY

In this section we sketch the derivation of the expression for the third-order nonlinear optical susceptibility χ_3, which we use in our analysis of the optical nonlinearities in the various regimes of quantum confinement. We denote by H the Hamiltonian of the unperturbed electron-hole Coulomb system in two-band approximation, and we treat the interaction between the system and the external field in dipole approximation. The total time-dependent Hamiltonian is then given as

$$H_t=H-P\mathcal{E}\cos(\omega t)\ , \tag{1}$$

where $\mathcal{E}$ is the applied electric field and P is the interband dipole moment operator (interband polarization). In rotation wave approximation we can write

$$\begin{aligned}P\cos(\omega t)&=(P_-+P_+)\cos(\omega t)\\&\simeq\tfrac{1}{2}(P_-e^{i\omega t}+P_+e^{-i\omega t})\ ,\end{aligned} \tag{2}$$

where P_+ and P_- are the polarization components corresponding to creation and annihilation of an electron-hole pair, respectively. Expanding the polarization in terms of electron and hole operators, one has

$$P_-=p_{cv}\sum_\sigma\int d\mathbf{x}\,\psi_{e\sigma}(\mathbf{x})\psi_{h\sigma}(\mathbf{x})\ , \tag{3}$$

where p_{cv} is the interband dipole matrix element $\psi_{e/h}$ is the annihilation operator for an electron or a hole, and σ is the spin index, respectively.

If one introduces a phenomenological decay constant γ, the Liouville equation for the density matrix ρ can be written as ($\hbar\equiv1$ in the remainder of this paper)

$$i\frac{\partial}{\partial t}\rho=[H_t(t),\rho]-i(\rho-\rho_0)\gamma\ , \tag{4}$$

with the initial condition

$$\rho\,|_{t=0}=\rho_0(H)\ , \tag{5}$$

where $\rho_0(H)$ is the unperturbed density matrix of the Hamiltonian H. In the following, we transform Eq. (4) into a form suitable for perturbative solutions. It is convenient to introduce the new operators

$$\begin{aligned}&\hat{\Omega}=\tfrac{1}{2}\hat{N}\omega\ ,\\&\hat{N}=\hat{N}_e+\hat{N}_h\ ,\\&\rho=e^{-i\hat{\Omega}t}e^{-i\tilde{H}t}\tilde{\rho}e^{i\tilde{H}t}e^{i\hat{\Omega}t}e^{-t\gamma}\ ,\\&\tilde{H}=H-\tfrac{1}{2}\mathcal{E}P-\hat{\Omega}\ ,\end{aligned} \tag{6}$$

where $\hat{N}_e$ and $\hat{N}_h$ are the number operators for electrons and holes, respectively. Assuming $[\hat{\Omega},\rho_0]=0$, Eq. (4) becomes

$$\frac{\partial\tilde{\rho}}{\partial t}=\gamma e^{i\tilde{H}t}\rho_0e^{-i\tilde{H}t}e^{t\gamma}\ , \tag{7}$$

with $\tilde{\rho}(0)=\rho_0$. The solution of Eq. (7) can be written as

$$\tilde{\rho}=\tilde{\rho}(0)+\gamma\int_0^t dt'\,e^{i\tilde{H}t'}\rho_0e^{-i\tilde{H}t'}e^{t'\gamma} \tag{8}$$

or, by using the definitions (6) and partial integration,

$$\begin{aligned}\rho=\rho_0-ie^{-i\hat{\Omega}t}\int_0^t dt'\,e^{(t'-t)\gamma}e^{i\tilde{H}(t'-t)}\\\times[\tilde{H},\rho_0]e^{-i\tilde{H}(t'-t)}e^{i\hat{\Omega}t}\ .\end{aligned} \tag{9}$$

In the present paper we are interested in the steady-state situation, $t\to\infty$, assuming that the external field is applied at $t=0$. Using Eq. (9) we obtain the expectation value of the polarization as

$$\langle P_{\pm}\rangle(t)=-\frac{i\mathcal{E}}{2}e^{\pm i\omega t}\times\int_{-\infty}^{0}dt'\,e^{t'\gamma}\mathrm{tr}(e^{i\tilde{H}t'}[\tilde{H},\rho_0]e^{-i\tilde{H}t'}P_{\pm})\ . \tag{10}$$

Since we are working in rotating wave approximation, the relation between the macroscopic polarization and the external electric field can be written in the form

$$\frac{1}{V}\langle P\rangle(t)=\tfrac{1}{2}(e^{i\omega t}\chi^{*}+e^{-i\omega t}\chi)\mathcal{E}\ , \tag{11}$$

where V is the crystal volume. Using Eqs. (9)–(11), we can extract the susceptibility as

$$\chi=\frac{i}{V}\int_{-\infty}^{0}dt'\,e^{t'\gamma}\langle[e^{-i\tilde{H}t'}P_{-}e^{i\tilde{H}t'},P]\rangle_0\ , \tag{12}$$

where $\langle\cdots\rangle_0$ denotes the average using ρ_0. Since we cannot evaluate Eq. (12) in closed form for most practical cases, we apply perturbative methods using the expansion

$$e^{\lambda(\hat{A}+\hat{B})}=e^{\lambda\hat{A}}\left[1+\int_0^{\lambda}d\lambda_1 e^{-\lambda_1\hat{A}}\hat{B}e^{\lambda_1\hat{A}}+\int_0^{\lambda}d\lambda_1\int_0^{\lambda_1}d\lambda_2 e^{-\lambda_2\hat{A}}\hat{B}e^{\lambda_2\hat{A}}e^{-\lambda_1\hat{A}}\hat{B}\times e^{\lambda_1\hat{A}}+\cdots\right], \tag{13}$$

where $\lambda=it$, $\hat{A}=H-\hat{\Omega}\equiv\tilde{H}_0$, $\hat{B}=-\mathcal{E}(P_{+}+P_{-})/2$ so that $\hat{A}+\hat{B}=\tilde{H}$. Truncating the expansion amounts to treating $\hat{B}$ perturbatively. Expanding Eq. (12) in powers of electric field we obtain the different orders of the optical susceptibility as

$$\begin{aligned}\chi_1&=-\frac{i}{V}\int_{-\infty}^{0}dt\langle[P(t),P_{-}(0)]\rangle_0 e^{t\gamma}\ ,\\ \chi_2&=0\ ,\\ \chi_3&=\frac{i\mathcal{E}^2}{4V}\int_{-\infty}^{0}dt_1\int_{-\infty}^{t_1}dt_2\int_{-\infty}^{t_2}dt_3\langle[P(t_3)[P(t_2),[P(t_1),P_{-}(0)]]]\rangle_0 e^{t_3\gamma}\ ,\end{aligned} \tag{14}$$

where

$$P(t)=e^{i\tilde{H}_0t}Pe^{-i\tilde{H}_0t}\ . \tag{15}$$

For the sake of simplicity, we now assume that the system is originally (at $t=0$) in its ground state, i.e., there are no electrons or holes before the laser field is applied. Furthermore, we restrict our basis of states to the energetically lowest electron-hole-pair state, which may be degenerate, $E_{1\delta}=E_1$ for all allowed δ. Under these conditions, Eq. (14) can be rewritten as

$$\chi_1=\frac{iA}{V}\frac{1}{i\omega_1+\gamma} \tag{16}$$

and

$$\chi_3=-\frac{i\mathcal{E}^2}{4V}\left\{\frac{4A^2}{(i\omega_1+\gamma)(\omega_1^2+\gamma^2)}-\sum_{\sigma}B_{\sigma}^2\left[\frac{2}{[i(\omega_{2\sigma}-\omega_1)+\gamma](\omega_1^2+\gamma^2)}+\frac{1}{(i\omega_1+\gamma)(i\omega_{2\sigma}+\gamma)}\left[\frac{1}{i(\omega_{2\sigma}-\omega_1)+\gamma}-\frac{1}{i\omega_1+\gamma}\right]\right]\right\}, \tag{17}$$

where

$$\begin{aligned}A&=\sum_{\lambda}|\langle 0|P_{-}|1\lambda\rangle|^2\ ,\\ B_{\sigma}&=\left|\sum_{\sigma}\langle 0|P_{-}|1\lambda\rangle\langle 1\lambda|P_{-}|2\sigma\rangle\right|\ ,\end{aligned} \tag{18}$$

and $\omega_1=E_1-\omega$ and $\omega_{2\sigma}=E_{2\sigma}-2\omega$. Here, E_1 and E_2 are the energies for the one-pair and two-pair states, respectively.

Equations (16)–(18) are the basic equations used in our further discussion. In the following sections of this paper, we evaluate the coefficients A and B, as well as the energies E_1 and E_2 for different regimes of quantum confinement.

III. THE REGIME OF WEAK QUANTUM CONFINEMENT

In this section we discuss the regime of weak quantum confinement, where the radius R of the quantum dots is much larger than the exciton Bohr radius in the corresponding bulk material. In this case, one may apply the so-called boson model to discuss the different electron-

hole-pair states. The boson model has been developed for bulk semiconductors and we first outline this case for later reference. Here, one treats the excitons as nonideal bosons which have two possible spin states: spin up and spin down, denoted as $\lambda=+1$ and -1, respectively. As a consequence of the van der Waals attraction between two excitons, an excitonic molecule or biexciton state may exist whose energy is reduced by the binding energy E_{xx} in comparison to the energy of a state with two excitons. In this paper, we consider only the biexciton singlet state.

We denote the one-pair state as

$$|1\lambda\rangle=e_\lambda^\dagger|0\rangle, \quad \lambda=\pm1 \tag{19}$$

where $e_\lambda^\dagger$ is the exciton creation operator and the two-electron-hole-pair state is

$$|2\rangle=\begin{cases} e_\lambda^\dagger e_{\lambda'}^\dagger|0\rangle & \text{for } \lambda\neq\lambda' \\ \frac{1}{\sqrt{2}}(e_\lambda^\dagger)^2|0\rangle & \text{for } \lambda=\lambda' , \end{cases} \tag{20}$$

with the energy

$$E_{2e}^0=2E_1 . \tag{21}$$

The biexciton state is

$$|b\rangle=b^\dagger|0\rangle , \tag{22}$$

where $b^\dagger$ is the biexciton creation operator, and the energy is

$$E_b^0=2E_i=E_{xx} . \tag{23}$$

In the boson model, both excitons and biexcitons are assumed to obey Bose commutation relations. Equation (3) then becomes particularly simple,

$$P_-=\sum_\lambda (p_{0e}e_\lambda+p_{eb}e^+_{-\lambda}b) , \tag{24}$$

where the vacuum-exciton dipole matrix element is

$$p_{0e}=p_{cv}\left[\frac{V}{\pi}a_B^3\right]^{1/2}$$

and the exciton-biexciton dipole matrix element p_{eb} is not volume dependent. Inserting Eq. (24) and the wave functions into Eq. (18), one obtains the coefficients A and B as

$$\begin{aligned} A^2&=4p_{0e}^4 \\ B^2&=2A^2 \end{aligned} \tag{25}$$

for the two-exciton state and

$$B^2=4p_{0e}^2p_{eb}^2 \tag{26}$$

for the biexciton state. Inserting (25) and (26) into (17) one sees that the contribution of the one-exciton state in χ_3 cancels exactly that of the two-exciton state, leaving only the contribution of the biexciton. From Eq. (16) we obtain

$$\chi_1=-\frac{2p_{cv}^2}{\pi a_B^3}\frac{1}{\omega-E_1+i\gamma} , \tag{27}$$

and Eq. (17) yields

$$\chi_3=-\frac{p_{cv}^2p_{eb}^2}{\pi a_B^3}\mathcal{E}^2\left[\frac{2}{(\omega-E_1)^2+\gamma^2}\frac{1}{\omega-E_1+E_{xx}+i\gamma}-\frac{E_{xx}/2}{(\omega-E_1+i\gamma)^2(\omega-E_1+E_{xx}/2+\gamma/2)(\omega-E_1+E_{xx}+i\gamma)}\right] . \tag{28}$$

Actually the boson model for bulk semiconductors allows the exact calculation of the full nonlinear susceptibility which we, however, do not need for the discussion in this paper.

In the remainder of this section we now discuss the modifications of the boson picture which arise in semiconductor microspheres under weak quantum confinement. Since the microsphere radius exceeds the exciton Bohr radius, it is reasonable to assume that the relative motion of the electrons and holes in the bound states (exciton and biexciton) is basically not influenced by the confinement. However, the center-of-mass motions of excitons and biexcitons are modified by the boundary conditions at the surface of the sphere. The corresponding quantization of the kinetic energies yields

$$E_b=E_b^0+\frac{1}{4(m_e+m_h)}(\pi/R)^2 \tag{29}$$

and

$$E_{2e}=E_{2e}^0+\frac{1}{m_e+m_h}(\pi/R)^2 , \tag{30}$$

showing that the spectral distance between the one- and two-photon absorption peaks varies as function of the microsphere radius. Moreover, the contributions of the one-exciton and two-exciton states to the third-order susceptibility do not compensate anymore. The confining geometry of a microsphere introduces deviations of the matrix elements from their bulk values given by Eqs. (25) and (26) and the idealized relationship, Eq. (21), between the energies of the one-exciton and two-exciton states does not hold anymore. These modifications are easy to understand if one keeps in mind that excitons and biexcitons in reality are not elementary bosons, but bound states of electrons and holes. Therefore, in a finite volume two excitons cannot be treated separately, but the Fermi nature of their components has to be taken into account. These arguments can be made quantitatively by writing the wave function of the exciton as

$$\Psi(\mathbf{x}_e,\mathbf{x}_h)=\Phi(\mathbf{x}_e-\mathbf{x}_h)\phi(\mathbf{X}) , \tag{31}$$

where $\mathbf{X}$ is the center-of-mass position of the exciton,

$$\mathbf{X}=\frac{m_e\mathbf{x}_e+m_h\mathbf{x}_h}{m_e+m_h}\ , \tag{32}$$

Φ is the ground-state wave function of the relative electron-hole motion (hydrogen wave function), and

$$\phi(\mathbf{X})=\Theta(R'-X)\left[\frac{\sin\pi X/R'}{\sqrt{2\pi R'}X}\right] \tag{33}$$

describes the motion of a particle in an infinite potential well of radius R', with $R'=R-a_B$ and Θ is the usual Heaviside unit step function.

Now one may construct the different spin states of two excitons using the wave functions (31)–(33). The singlet state is

$$|e_\downarrow h_\downarrow,e_\uparrow h_\uparrow\rangle=\int dx_{e_1}\int dx_{e_2}\int dx_{h_1}\int dx_{h_2}\,\Psi(x_{e_1},x_{h_1})\Psi(x_{e_2},x_{h_2})\hat{\psi}^\dagger_{e\uparrow}(x_{e_1})\hat{\psi}^\dagger_{e\downarrow}(x_{e_2})\hat{\psi}^\dagger_{h\uparrow}(x_{h_1})\hat{\psi}^\dagger_{h\downarrow}(x_{h_2})|0\rangle \tag{34}$$

and the (double degenerate) triplet state is

$$|e_\uparrow h_\uparrow,e_\uparrow,h_\uparrow\rangle=\frac{1}{N}\int dx_{e_1}\int dx_{e_2}\int dx_{h_1}\int dx_{h_2}\,\Psi(x_{e_1},x_{h_1})\Psi(x_{e_2},x_{h_2})\hat{\psi}^\dagger_{e\uparrow}(x_{e_1})\hat{\psi}^\dagger_{e\uparrow}(x_{e_2})\hat{\psi}^\dagger_{h\uparrow}(x_{h_1})\hat{\psi}^\dagger_{h\uparrow}(x_{h_2})|0\rangle\ , \tag{35}$$

with the normalization factor

$$N=\sqrt{2}-\left[2\int dx_{e_1}\int dx_{e_2}\int dx_{h_1}\int dx_{h_2}\,\Psi(x_{e_1},x_{h_1})\Psi(x_{e_1},x_{h_2})\Psi(x_{e_2},x_{h_1})\Psi(x_{e_2},x_{h_2})\right]^{1/2}\ . \tag{36}$$

Estimates for the radius dependent corrections of the coefficients A and B and of singlet and triplet energies can be obtained using Eqs. (31)–(36). These calculations are straightforward but lengthy and we suppress the details here. As a result of the discussed modifications, one finds that the nonlinear contributions around the exciton resonance do not vanish anymore, as they do in the bulk limit.

A word of caution should be mentioned here regarding the bulk limit $R\to\infty$. When considering electron-hole systems in bulk semiconductors it is actually not correct to keep only the lowest energy levels when computing the nonlinear optical response. The contributions of the excited levels become more and more important. Therefore, when using our Eq. (17) we do not have a description which approaches asymptotically the correct infinite volume limit. To obtain the correct limiting behavior one has include the contributions of increasingly many energy levels.

IV. THE REGIME OF MODERATE QUANTUM CONFINEMENT

The regime of moderate quantum confinement is defined as the situation, where the radius of the quantum dot is smaller than the electron Bohr radius but larger than the hole Bohr radius,

$$a_h<R<a_e\ . \tag{37}$$

This situation is very relevant for most direct-gap semiconductors because of the large difference between the effective masses of electrons and holes. To model the situation of moderate quantum confinement, we assume that the confinement dominates the motion of the electrons, but the Coulomb forces are still important for the motion of the holes. Effectively the holes move in the cloud of the strongly confined electrons which, hence, produce a mean Coulomb potential.

In order to deal with Coulomb effects, we assume semiconductor quantum dots with the background dielectric constant ϵ_2 which are embedded in a material with background dielectric constant ϵ_1. The full Coulomb interaction between two point charges in this case consists of the Coulomb interaction between the particles inside the sphere plus an additional term caused by the induced surface charge of the sphere,[5]

$$V(\mathbf{x}_1,\mathbf{x}_2)\,|_R=V(\mathbf{x}_1,\mathbf{x}_2)\,|_{R=\infty}+\delta V(\mathbf{x}_1,\mathbf{x}_2)$$

$$=\pm\frac{e^2}{\epsilon_2|\mathbf{x}_1-\mathbf{x}_2|}+\delta V(\mathbf{x}_1,\mathbf{x}_2)\ , \tag{38}$$

where the positive (negative) sign is for equal (opposite) charges. The modification of the Coulomb potential has been discussed by Brus[5] and the results relevant to our calculations are summarized in the Appendix of this paper.

To compute the coefficients for the third-order optical susceptibility, we need the wave functions and energy eigenvalues of the one- and two-pair states. Since we assume strongly quantum confined electrons, the electron wave function is simply

$$\phi_e(x_e)=\frac{1}{\sqrt{2\pi R}}\frac{\sin(\pi x_e/R)}{x_e} \tag{39}$$

and we compute the motion of the hole in the average electron potential.

A. The one-pair state

First we analyze the one-pair state. The effective Schrödinger equation for the hole is

$$\left[-\frac{1}{2m_h}\nabla_h^2+\int d\mathbf{x}_e\phi_e^2(\mathbf{x}_e)V(\mathbf{x}_e,\mathbf{x}_h)\Big|_R-E_{1h}\right]\times\Phi_h(x_h)=0\ . \tag{40}$$

Since we are dealing with quantum-dot sizes fulfilling the condition (41), we use the expansion[4]

$$\frac{e^2}{\epsilon_2}\int d\mathbf{x}_e \frac{\phi_e^2(x_e)}{|\mathbf{x}_e-\mathbf{x}_h|} \simeq \frac{4a_B E_R}{R}\left[\int_0^1 dx \frac{\sin^2\pi x}{x}-\frac{\pi^2}{6}\left[\frac{x_h}{R}\right]^2+\cdots\right], \tag{41}$$

where terms with odd powers disappear for symmetry reasons. Inserting (41) into (40) and using Eq. (A9) yields

$$\left[-\frac{1}{2m_h}\nabla_h^2+\left[\frac{2\pi^2 E_R a_B}{3R^3}+\frac{\alpha_1 e^2}{2R^3}\right]x_h^2-E'_{1h}\right]\times\Phi_h(x_h)=0 . \tag{42}$$

where the expressions for α_n is given in the Appendix [(A7)] and

$$E'_{1h}=E_{1h}+\Delta E ,$$

ΔE being given by Eq. (A10) and only terms up to order $(x_h/R)^3$ have been kept. Equation (42) is the Schrödinger equation for the harmonic oscillator. If we replace the boundary condition at the surface of the sphere, $\Phi(x=R)=0$, with the boundary conditions at ∞, $\Phi(x=\infty)=0$, we obtain the eigenfunction of (42) as

$$\Phi_h(x_h)=\frac{1}{\pi^{3/4}x_{01}^{3/2}}e^{-x_h^2/x_{01}^2} , \tag{43}$$

and the energy eigenvalue is

$$E_1=E_{1h}+E_{1e}=\frac{1}{2m_e}\left[\frac{\pi}{R}\right]^2+\frac{4a_B E_R}{R}\left\{-\int_0^1 dx\frac{\sin^2(\pi x)}{x}+\frac{3}{4}\left[\left[\frac{4\pi^2}{9}+2\epsilon'\right]\frac{a_h}{R}\right]^{1/2}\right\}, \tag{44}$$

where

$$\frac{x_{01}}{R}=\left[\frac{a_h/R}{2\pi^2/3+2\epsilon'}\right]^{1/4} \tag{45}$$

and

$$\epsilon'=\frac{\epsilon_2/\epsilon_1-1}{\epsilon_2/\epsilon_1+2} . \tag{46}$$

Since the hole is strongly localized around the center, the violation of the boundary condition at the surface of the sphere turns out to be very insignificant, as we have verified by comparison of the approximate results (43) and (44) with numerical solutions of Eq. (42).

B. The two-pair states

We consider here the lowest two-pair state, which is a Coulomb-correlated ("bound") state. Unlike the case of weak quantum confinement, in the presently discussed regime of moderate confinement, one cannot have a two-pair state of relatively independent excitons. In the discussion of this correlated two-pair state, we use the same approximations as in the case of the one-pair state. It is easy to see that there is only one possible spin combination for the two-pair state, in which the sum of the electron (hole) spins is zero. Because of the strong electron confinement, the two-electron wave function can simply be approximated as the product of the single-electron wave functions, Eq. (39). The two holes are subject to the combined fields of the electrons and the surface charge

$$\left[-\frac{1}{2m_h}\left[\nabla_{h_1}^2+\nabla_{h_2}^2\right]+\int d\mathbf{x}_{e_1}\int d\mathbf{x}_{e_1}\phi_e^2(\mathbf{x}_{e_1})\phi_e^2(\mathbf{x}_{e_2})\times V(\mathbf{x}_{e_1},\mathbf{x}_{e_2},\mathbf{x}_{h_1},\mathbf{x}_{h_2})|_R-E_{2h}\right]\phi_{2h}(\mathbf{x}_{h_1},\mathbf{x}_{h_2})=0 . \tag{47}$$

The total Coulomb potential $V(x_1,x_2,x_3,x_4)$ for the interaction of the two electrons and the two holes is discussed in the Appendix. We separate the wave function $\phi(\mathbf{x}_{h_1},\mathbf{x}_{h_2})$ into a part ζ describing the center-of-mass motion and a part Φ describing the relative motion,

$$\phi_{2h}(\mathbf{x}_{h_1},\mathbf{x}_{h_2})=\Phi(\mathbf{x})\zeta(\mathbf{X}) . \tag{48}$$

with $\mathbf{X}=(\mathbf{x}_{h_1}+\mathbf{x}_{h_2})/2$ and $\mathbf{x}=\mathbf{x}_{h_1}-\mathbf{x}_{h_2}$.

Inserting (48) and (47) and using (A12)–(A15), we obtain for the center-of-mass motion

$$\left[-\frac{1}{4m_h}\nabla_X^2+\left[\frac{4\pi^2e^2}{3R^3\epsilon_2}+\frac{6\epsilon' a_B E_R}{R^3}\right]X^2\right]\zeta(\mathbf{X})=e_{\rm cm}\zeta(\mathbf{X}) , \tag{49}$$

with the solution

$$\zeta(\mathbf{X})=\frac{1}{\pi^{3/4}x_{02}^{3/2}}e^{-0.5(X/x_{02})^2} , \tag{50}$$

$$e_{\rm cm}=\frac{3a_B E_R}{2R}\left[\frac{a_h}{R}\left[\frac{16\pi^2}{3}+12\epsilon'\right]\right]^{1/2} , \tag{51}$$

where

$$\frac{x_{02}}{R}=\left[\frac{a_h}{R(16\pi^2/3+12\epsilon')}\right]^{1/4} .$$

For the relative motion, the Schrödinger equation resulting from Eq. (47) is

$$\left[-\frac{1}{m_h}\nabla_x^2+V_{re}(x)\right]\Phi(\mathbf{x})=e_{re}\Phi(\mathbf{x}) , \tag{52}$$

where

$$V_{re}(x)=\left[\frac{\pi^2e^2}{3R^3\epsilon_2}+\frac{\epsilon' a_B E_R}{2R^3}\right]x^2+\frac{e^2}{\epsilon_x x} . \tag{53}$$

To obtain an analytic solution, we expand the potential V_{re} around its minimum,

$$x_{\min}=\frac{R}{(2\pi^2/3+1/2\epsilon')^{1/3}} .$$

Keeping terms up to second order, Eq. (52) becomes

$$\left\{-\frac{\partial^2}{\partial\xi^2}+\left[m_h R\left[\frac{\pi^2 e^2}{3\epsilon_2}+\frac{\epsilon' a_B E_R}{2}\right]+\frac{e^2}{\epsilon_2\xi_0^3}\right](\xi-\xi_0)^2\right\}U(\xi)=(e'_{re}-e_0)U(\xi) , \tag{54}$$

where we have introduced the new variables

$$\xi=\frac{x}{R},\quad \xi_0=\frac{x_{\min}}{R},\quad \Phi=\frac{U}{x} ,$$

$$e_0=3E_R\frac{a_B}{R}(2\pi^2/3+1/2\epsilon')^{1/3} ,$$

$$e_{re}=e'_{re}2E_R\frac{a_B a_h}{R^2} .$$

Equation (54) is the Schrödinger equation for the shifted harmonic oscillator which has the parabolic cylinder functions as eigenfunctions

$$U(\xi)=c_p D_p\left[4\frac{R}{a_h}(\pi^2+\tfrac{3}{4}\epsilon')^{1/4}(\xi-\xi_0)\right] , \tag{55}$$

and the energy eigenvalues are

$$e'_{re}=e'_0+(2p+1)[(R/a_h)(\pi^2+0.75\epsilon')]^{1/2} . \tag{56}$$

The parameter p has to be determined from the boundary condition $U_p(\xi=0)=0$ and the normalization constant c_p is obtained from the condition

$$\int_0^2 d\xi\, U^2(\xi)=1 .$$

The two-pair state can be expressed as

$$|2\rangle=\int dx_{e_1}\int dx_{e_2}\int dx_{h_1}\int dx_{h_2}\,\phi_e(\mathbf{x})\phi_e(\mathbf{x})\Phi(\mathbf{x}_{h_1},\mathbf{x}_{h_2})\psi^\dagger_{e\uparrow}\psi^\dagger_{e\downarrow}\psi^\dagger_{h\uparrow}\psi^\dagger_{h\downarrow}|0\rangle . \tag{57}$$

Adding up all the contributions to the energy, we obtain

$$\frac{E_2}{E_R}=2\pi^2(a_e/R)^2+\frac{a_B}{R}\{-15.6+3(2\pi^2/3+0.5\epsilon')^{1/3}+(a_h/R)^{1/2}[(4\pi^2+3\epsilon')^{1/2}+3(4\pi^2/3+3\epsilon')^{1/2}]\} . \tag{58}$$

The number 15.6 is the computed result of the expression

$$\frac{e^2}{\epsilon_2}\int d\mathbf{x}_{e_1}\int d\mathbf{x}_{e_2}\frac{\phi_e^2(x_{e_1})\phi_e^2(x_{e_2})}{|\mathbf{x}_{e_1}-\mathbf{x}_{e_2}|}\simeq 15.6E_R .$$

The numerical evaluation shows that for realistic semiconductor parameters the energy difference E_2-2E_1 is positive in the moderate-confinement regime. For the simplified case of $\epsilon_2=\epsilon_1$, evaluation of the terms in Eqs. (44) and (58) yields

$$E_2-2E_1\simeq E_R\frac{a_B}{R}\left[1.8\left[\frac{a_h}{R}\right]^{1/2}-0.4\right] .$$

The two-electron-hole-pair state, which we may loosely call the quantum-confined "biexciton", has a higher energy than twice the one-electron-hole-pair state ("exciton"). This is in contrast to bulk semiconductors, where the Coulomb attraction between electrons and holes overcompensates the electron-electron and hole-hole repulsion, leading to a biexciton state whose energy is that of the two-exciton state *minus* the biexciton binding energy. However, in the case of sufficiently small microcrystallites, the quantum confinement for two holes is stronger than that for a single hole. This increased quantum confinement is indirectly a consequence of the Coulomb repulsion between the two holes, which forces them to be somewhat displaced from the center of the sphere, in contrast to the single hole, which always stays close to the center. As a consequence of the confinement, the two-electron-two-hole complex cannot rearrange itself to reduce the repulsive forces between the two holes and, hence, the total energy increases.

C. Evaluation of the optical susceptibility

Using the expressions derived in Secs. IV A and IV B, we are now in the position to obtain the matrix elements entering Eqs. (17) for the nonlinear susceptibility χ_3. Using Eqs. (45) and (46), it is found that

$$\langle 0|P|1\rangle=2^{3/2}/\pi^{1/4}p_{cv}(R/a_h)^{3/8}(2\pi^2/3+2\epsilon')^{3/8}\times\int_0^1 dr\, r\sin(\pi r)e^{-0.5r^2(2\pi^2/3+2\epsilon')^{1/2}(R/a_h)^{1/2}} . \tag{59}$$

The other matrix element is

$$\langle 1\lambda \mid P \mid 2\rangle = \frac{8p_{cv}}{(2\pi)^{1/2}} \frac{(R/x_{02})^{3/2}(R/x_{01})^{3/2}}{(R/x_0)^2+0.5(R/x_{01})^2} \times \int_0^1 dx \sin(\pi x) e^{-0.5[(R/x_{02})^2+(R/x_0)^2]x^2} \times \int_0^2 dy\, e^{-0.5[(R/x_{02})^2+0.25(R/x_{01})^2]y^2} \sin\{[(R/x_{02})^2+0.5(R/x_{01})^2]xy\}U(y) . \quad (60)$$

Inserting the results (44) and (58)–(60) into Eqs. (17) and (18) we can now evaluate the nonlinear susceptibility χ_3 for the regime of intermediate quantum confinement. Defining

$$\tilde{\chi}_3 = \chi_3 \frac{4\pi}{3} R^3 \frac{E_R^2}{p_{cv}^4 \mathcal{E}^2} , \quad (61)$$

we introduce a normalized susceptibility $\tilde{\chi}_3$, which depends only weakly on material parameters.

As a typical example of the results for the regime of moderate quantum confinement we show in Fig. 1 the imaginary part [Fig. 1(a)] and the real part [Fig. 1(b)] of $\tilde{\chi}_3$ for three different values of the damping constant γ. For this figure we have chosen $\epsilon_2/\epsilon_1=10$, which is typical for semiconductor microspheres surrounded by air or by glass, and $a_h/a_e=0.2$. We see in Fig. 1(a) that the imaginary part of $\tilde{\chi}_3$ exhibits a positive and a negative resonance. The negative resonance occurs at $\omega=E_1$ describing the saturation of the one-pair transition (bleaching of the exciton resonance). The positive resonance occurs roughly at $\omega=E_2/2$. Since the imaginary part of the susceptibility is directly proportional to the absorption coefficient α of the semiconductor material, a positive $\tilde{\chi}_3$ describes absorption which increases with increasing light intensity. The positive resonance around $E_2/2$ is therefore reminiscent of the induced absorption resonance (biexciton resonance) in bulk semiconductors.[21,22] However, in contrast to bulk semiconductors, in the microspheres the positive resonance of $\tilde{\chi}_3$ occurs on the high-energy side of the one-pair resonance. This is a direct consequence of the quantum confinement which, as discussed at the end of Sec. IV B, causes $E_2/2>E_1$. The real part of $\tilde{\chi}_3$ exhibits a somewhat more complicated structure with a strong positive peak occurring at the energy in between the negative and positive resonances of $\mathrm{Im}\tilde{\chi}_3$. This positive peak is due to the fact that a decreasing-absorption peak has a positive dispersive peak on its high-energy side and an increasing-absorption peak has a positive dispersive peak on its low-energy side. Hence, both positive contributions add up in $\mathrm{Re}\,\tilde{\chi}_3$, giving rise to the strong positive resonance. Both on the high-energy side and on the low-energy side of the positive resonance $\mathrm{Re}\tilde{\chi}_3$ exhibits negative resonances. The results for the different damping constants γ in curves 1–3 show the general trend that the magnitude of the nonlinearities is strongly reduced with increasing γ and the width (FWHM) of the structures increases.

To study the influence of the surface polarization of the microspheres, we have evaluated $\tilde{\chi}_3$ also for $\epsilon_2/\epsilon_1=1$. The resulting spectra are quite similar to those shown in Fig. 1. Most notably, the absence of surface polarization effects causes the separation between the negative and positive resonances in $\mathrm{Im}\tilde{\chi}_3$ to increase by approximately 50%, whereas the magnitude of the peaks decreases by less than 10%. These observations indicate that the surface polarization modifies the energy difference E_2-2E_1 but changes the matrix elements only slightly.

More pronounced modifications of the $\tilde{\chi}_3$ spectra are obtained when changing the ratio of the electron and hole Bohr radii. In Fig. 2 we show results which have been computed for the same conditions as Fig. 1 but choosing $a_h/a_e=0.1$. The comparison reveals that the overall structure of $\tilde{\chi}_3$ remains unchanged, but the smaller ratio a_h/a_e causes an increasing energy difference E_2-2E_1 which leads to a wider separation between the positive and negative resonances in $\mathrm{Im}\tilde{\chi}_3$. At the same time, we

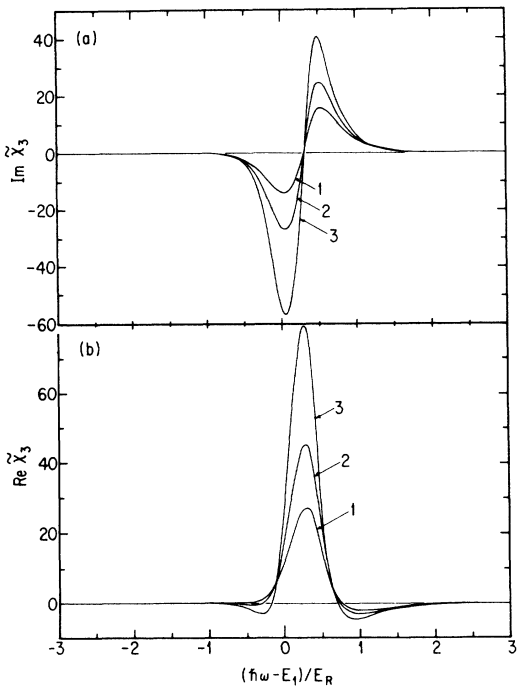

FIG. 1. Imaginary part (a) and the real part (b) of the normalized third-order susceptibility $\tilde{\chi}_3$ in the regime of moderate quantum confinement vs energy for three different values of the damping constant. $\gamma/E_R=0.6$ (1), 0.5 (2), 0.4 (3). Here, E_1 is the energy of the one-electron-hole-pair state and E_R is the binding energy of the exciton in the bulk semiconductor material. The other parameters are $\epsilon_2/\epsilon_1=10$ and $a_h/a_e=0.2$, where, respectively, ϵ_1 and ϵ_2 are the background dielectric constants of the surrounding medium and of the semiconductor, and $a_{e/h}$ is the Bohr radius of the electron or hole in the semiconductor microcrystallite.

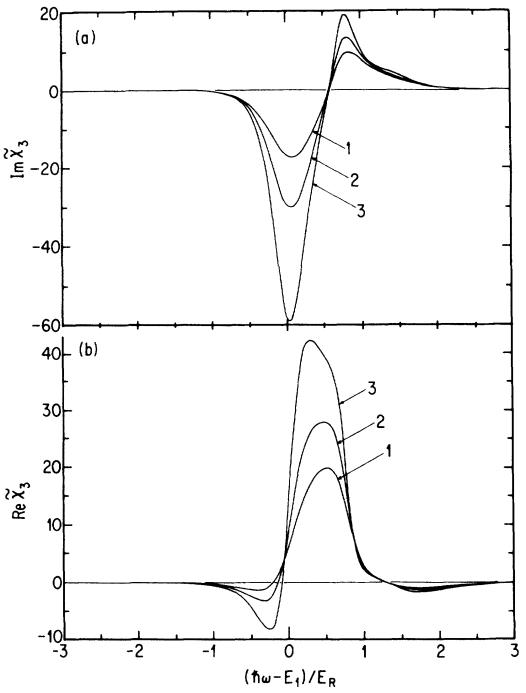

FIG. 2. Same as Fig. 1 but $a_h/a_e = 0.1$.

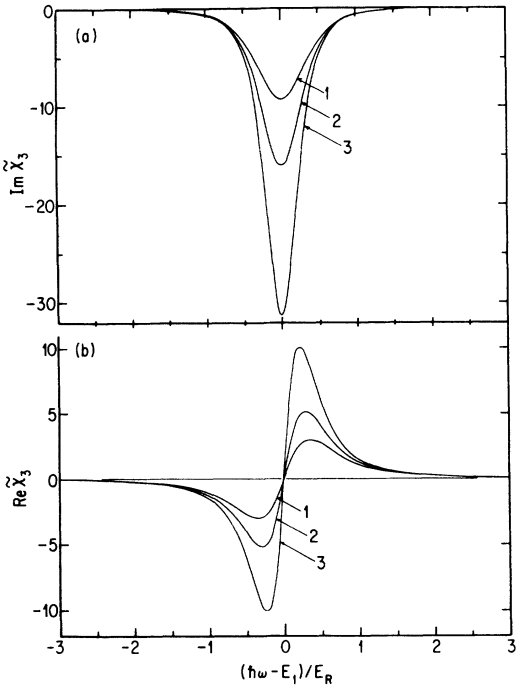

FIG. 3. Same as Fig. 1 but for the regime of strong quantum confinement.

observe a reduction of the positive peak in $\mathrm{Re}\tilde{\chi}_3$ and an increase of the negative resonance for $\omega < E_1$ [Fig. 2(b)], which becomes larger than that in Fig. 1(b).

V. THE REGIME OF STRONG QUANTUM CONFINEMENT

If one considers microcrystallites whose radii R are much smaller than the Bohr radii of electrons and holes in the corresponding bulk material (quantum dots), the confinement energy is the dominant energy contribution. In this case, the Coulomb potential may be neglected in comparison with the large kinetic energy caused by the strong quantum confinement. Consequently, the two electrons and holes in the two-pair ground state have to have opposite spins thus removing the degeneracy. The wave functions for the single-pair and two-pair ground states are

$$\begin{aligned} |1\lambda\rangle &= a_{e\sigma}^{\dagger} a_{h\sigma}^{\dagger} |0\rangle, \quad \sigma = \uparrow, \downarrow ; \\ |2\rangle &= a_{e\downarrow}^{\dagger} a_{e\uparrow}^{\dagger} a_{h\downarrow}^{\dagger} a_{h\uparrow}^{\dagger} |0\rangle , \end{aligned} \tag{62}$$

where $E_1 = 1/2\mu(\pi/R)^2 + E_{\mathrm{gap}}$, $E_2 = 2E_1$, and μ is the reduced mass of the exciton, $1/\mu = 1/m_e + 1/m_h$. Inserting (62) into (18), one obtains the coefficients A and B as

$$A = B = 2p_{cv}^2 \tag{63}$$

and the susceptibility from Eqs. (16) and (17) as

$$\begin{aligned} \chi_1(\omega) &= -\frac{3}{2\pi}\frac{p_{cv}^2}{R^3}\frac{1}{\omega - E_1 + i\gamma} \\ \chi_3(\omega) &= \frac{3}{2\pi}\frac{p_{cv}^4}{R^3}\mathcal{C}^2\left[\frac{1}{\omega - E_1 + i\gamma}\frac{1}{(\omega - E_1)^2 + \gamma^2}\right] . \end{aligned} \tag{64}$$

Actually, for the regime of strong quantum confinement, one can easily calculate even the full nonlinear optical susceptibility,[19] since the energetically lowest optical transition of the semiconductor in this case is essentially that of a two-level system.[23] We evaluate Eq. (64) in this paper only to have a systematic comparison with the results in the other quantum-confinement regimes.

Introducing again the normalized third-order susceptibility $\tilde{\chi}_3$ (Eq. 61), we plot the resulting spectra in Fig. 3. The imaginary part of $\tilde{\chi}_3$ [Fig. 3(a)] is strictly negative and resonates at the one-photon transition energy E_1, indicating the saturation of the one-pair resonance. The real part of $\tilde{\chi}_3$ in Fig. 3(b) shows the simple dispersive structure corresponding to the saturating absorption in Fig. 3(a). The additional structures present in Figs. 1 and 2 are absent in Fig. 3 since the Coulomb effects are negligible in the regime of strong quantum confinement.

VI. DISCUSSION

The analysis presented in this paper shows that the lifting of the degeneracy of the two-pair state leads to a nonvanishing third-order susceptibility in the regimes of moderate and strong quantum confinement. In both cases, we observe resonating behavior of χ_3 at the one-pair energy E_1 with additional resonances in the case of moderate quantum confinement due to the interplay of Coulomb and confinement effects.

So far, we have discussed our results in terms of the almost material parameter independent quantity $\tilde{\chi}_3$ introduced in Eq. (61). To obtain estimates of the expected optical nonlinearities in real semiconductor materials we have to evaluate the changes $\Delta\alpha$ of the absorption coefficient and the changes Δn of the refractive index.

The absorption change is

$$\Delta\alpha=\frac{4\pi\omega}{c\sqrt{\epsilon_2}}\mathrm{Im}\chi_3 \tag{65}$$

and the refractive index change is

$$\Delta n=\frac{2\pi}{\sqrt{\epsilon_2}}\mathrm{Re}\chi_3 \ . \tag{66}$$

In terms of the normalized susceptibility $\tilde{\chi}_3$, we therefore have

$$\frac{\Delta\alpha}{I}=\frac{24\pi 10^{13}}{c^2}\epsilon_2^{3/2}\frac{a_B^6}{R^3}\frac{\omega E_R}{E_g^2}\mathrm{Im}\tilde{\chi}_3\equiv\kappa_1\frac{a_B^3}{R^3}\mathrm{Im}\tilde{\chi}_3 \tag{67}$$

and

$$\frac{\Delta n}{I}=\frac{12\pi 10^{13}}{c}\epsilon_2\frac{a_B^6}{R^3}\frac{E_R}{E_g^2}\mathrm{Re}\tilde{\chi}_3\equiv\kappa_2\frac{a_B^3}{R^3}\mathrm{Re}\tilde{\chi}_3 \ , \tag{68}$$

where I is the light intensity inside the microspheres in units MW/cm^2. To obtain Eqs. (67) and (68) we have used the well-known relation between the dipole matrix element and the semiconductor band gap, $p_{cv}=\hbar e/\sqrt{4\mu E_g}$, obtained in $k\cdot p$ perturbation theory. (The factor 10^{13} enters because of the conversion of $\mathcal{E}^2$ into light intensity I in units of MW/cm^2).

As a consequence of the fact that the strongest material dependence in (67) and (68) is in terms of the bulk-exciton Bohr radius, it is clear that semiconductor materials with large Bohr radii are the best candidates for strong nonlinearities. To compare different semiconductors we choose the representative examples GaAs, CdS, and CuCl. The relevant material parameters are

	E_g (eV)	E_R (meV)	a_B(Å)	$m_e(m_0)$	$m_h(m_0)$
GaAs	1.519	4.2	124	0.0665	0.52
CdS	2.583	27	30.1	0.235	1.35
CuCl	3.354	152	7.5	0.5	2

where m_0 is the free-electron mass. Evaluating the prefactors κ_1 and κ_2 which scale the absorptive and dispersive changes, we obtain

	κ_1 (cm^{-1})	κ_2
GaAs	181	1.18×10^{-3}
CdS	6.0	2.3×10^{-5}
CuCl	0.223	6.88×10^{-6}

indicating that the expected nonlinear changes in GaAs are substantially larger than in the other two materials.

Equations (67) and (68) show that there is the additional factor a_B^3/R^3 scaling both $\Delta\alpha$ and Δn. Even though a comparison between Figs. 1 and 3 indicates that the magnitude of $\tilde{\chi}_3$ in the regime of moderate quantum confinement is larger than in the strong-confinement regime, the factor a_B^3/R^3 causes us to expect the largest nonlinearities for strong quantum confinement. However, in practice it seems to be exceedingly complicated to realize microstructures exhibiting strong quantum confinement using materials like CdS or CuCl, or even GaAs. In terms of numbers, the radius of such structures would have to be less than approximately 14 Å in GaAs, less than approximately 4.5 Å in CdS, and less than approximately 1.5Å in CuCl. Besides the complication of fabricating such truly microscopic structures, it seems to be very doubtful that the theoretical description in terms of semiconductors with bands and effective masses can still be applied. In this sense, we have included the analysis of the regime of strong quantum confinement only for comparison.

Because of the large difference between the effective masses of electrons and holes, the requirements for moderate quantum confinement are far less stringent than those for strong confinement, and some structures in this moderate-confinement regime have already been produced. However, another parameter which is extremely important in determining the magnitude of the expected nonlinearities in all regimes of quantum confinement is the broadening factor γ. The different curves in Figs. 1–3 show the rapid decrease of the nonlinearities with increasing γ. So far, we have only been discussing homogeneous broadening. Additionally, however, one also has to worry about inhomogeneous broadening, which is mainly caused by the size distribution of the microcrystallites. Our analysis of inhomogeneous broadening will be discussed in another publication. Here we only want to emphasize that we expect a strong reduction of the optical nonlinearities for an increasing width of the particle size distribution. This leads us to the conclusion that achieving a narrow size distribution is probably the most important, certainly also the most challenging task in the production of actual semiconductor microstructures.

ACKNOWLEDGMENTS

This work has been supported by the Optical Circuitry Cooperative, Optical Sciences Center, University of Arizona and by NATO (Travel Grant No. 87/0736). A grant for computer time at the John von Neuman Computer Center, Princeton, is gratefully acknowledged.

APPENDIX: THE COULOMB PROBLEM IN SEMICONDUCTOR QUANTUM DOTS

As shown by Brus,[5] the Coulomb interaction between two point charges in a semiconductor microsphere of radius R with background dielectric constant ϵ_2 embedded in a material with background dielectric constant ϵ_1 is

$$V(\mathbf{x}_1,\mathbf{x}_2)\,|_R=V(\mathbf{x}_1,\mathbf{x}_2)\,|_{R=\infty}+\delta V(\mathbf{x}_1,\mathbf{x}_2) \ , \tag{A1}$$

where the additional term is caused by the induced surface charge of the sphere. According to Ref. 5, δV can be written as

$$\delta V(\mathbf{x}_1,\mathbf{x}_2)=Q_1(\mathbf{x}_1)+Q_1(\mathbf{x}_2)\mp Q_2(\mathbf{x}_1,\mathbf{x}_2) \ , \tag{A2}$$

where $-$ $(+)$ is for charges with opposite (equal) sign. The different terms in (A2) are

$$Q_1(\mathbf{x})=\sum_{n=0}^{\infty}Q_{1,n}(x) \ , \tag{A3}$$

with

$$Q_{1,n}(x)=\frac{e^2}{2R}\alpha_n(x/R)^{2n} , \tag{A4}$$

and

$$Q_2(\mathbf{x}_1,\mathbf{x}_2)=\sum_{n=0}^{\infty} Q_{2,n}(\mathbf{x}_1\mathbf{x}_2) , \tag{A5}$$

with

$$Q_{2,n}(\mathbf{x}_1,\mathbf{x}_2)=\alpha_n\frac{e^2}{R}\left[\frac{\mathbf{x}_1\mathbf{x}_2}{R^2}\right]^n P_n(\cos(\theta)) , \tag{A6}$$

where θ is the angle between $\mathbf{x}_1$ and $\mathbf{x}_2$, P_n is the nth-order Legendre polynomial and

$$\alpha_n=\frac{(\epsilon_2/\epsilon_1-1)(n+1)}{\epsilon_2(n\epsilon_2/\epsilon_1+n+1)} . \tag{A7}$$

In the main part of this paper, we need the Coulomb potential averaged with the spherically symmetric wave function, Eq. (39). Considering the expression

$$\int d\mathbf{x}_e\phi_e^2(x_e)\delta V(\mathbf{x}_e,\mathbf{x}_h)$$

entering Eq. (40), we see that only the term $Q_{2,0}$ in Q_2, Eq. (A5), gives a contribution since the integral over the nth-order Legendre polynomial vanishes for all $n\neq 0$. Furthermore,

$$Q_{2,0}(x_e,x_h)=Q_{1,0}(x_e)+Q_{1,0}(x_h) , \tag{A8}$$

leaving only the contributions of $Q_{1,n}(x_e)+Q_{1,n}(x_h)$, $n\geq 1$. Expanding in terms of (x_h/R) and keeping terms up to third order, we obtain

$$\int d\mathbf{x}_e\phi_e^2(x_e)\delta V(\mathbf{x}_e,\mathbf{x}_h)\simeq\frac{\alpha_1 e^2}{2R^3}x_h^2+\Delta E , \tag{A9}$$

where ΔE is independent of x_h, introducing merely an energy shift

$$\Delta E=\sum_{n=1}^{\infty}\int d\mathbf{x}_e\phi_e^2(x_e)Q_{1,n}(x_e)=\frac{2a_B}{R}E_R c(\epsilon_2/\epsilon_1) , \tag{A10}$$

with

$$c(\epsilon)=\sum_{n=1}^{\infty}\frac{(\epsilon-1)(n+1)}{\epsilon n+n+1}\int_0^1 dx\,\sin^2(\pi x)x^{2n} . \tag{A11}$$

Equations (A9)–(A12) are used in Eq. (42).

Considering the four-particle Coulomb terms entering Eq. (47), we use a separation like (A1),

$$V(\mathbf{x}_{e_1},\mathbf{x}_{e_2},\mathbf{x}_{h_1},\mathbf{x}_{h_2})\,|_R=V(\mathbf{x}_{e_1},\mathbf{x}_{e_2},\mathbf{x}_{h_1},\mathbf{x}_{h_2})\,|_{R=\infty}+\delta V(\mathbf{x}_{e_1},\mathbf{x}_{e_2},\mathbf{x}_{h_1},\mathbf{x}_{h_2}) , \tag{A12}$$

where

$$\begin{aligned}V(\mathbf{x}_{e_1},\mathbf{x}_{e_2},\mathbf{x}_{h_1},\mathbf{x}_{h_2})\,|_{R=\infty}&=V(\mathbf{x}_{h_1},\mathbf{x}_{h_2})\,|_{R=\infty}+V(\mathbf{x}_{e_1},\mathbf{x}_{h_1})\,|_{R=\infty}\\&+V(\mathbf{x}_{e_1},\mathbf{x}_{h_2})\,|_{R=\infty}+V(\mathbf{x}_{e_2},\mathbf{x}_{h_1})\,|_{R=\infty}\\&+V(x_{e_2},x_{h_2})\,|_{R=\infty}+V(\mathbf{x}_{e_1},\mathbf{x}_{e_2})\,|_{R=\infty}\end{aligned} \tag{A13}$$

is just the sum of the bulk Coulomb potentials. The correction term is

$$\begin{aligned}\delta V(x_{e_1},x_{e_2},x_{h_1},x_{h_2})&=Q_1(x_{e_1})+Q_1(x_{e_2})+Q_1(x_{h_1})+Q_1(x_{h_2})\\&+Q_2(x_{e_1},x_{e_2})+Q_2(x_{h_1},x_{h_2})-Q_2(x_{e_1},x_{h_1})\\&-Q_2(x_{e_1},x_{h_2})-Q_2(x_{e_2},x_{h_1})-Q_2(x_{e_2},x_{h_2}) .\end{aligned} \tag{A14}$$

In Eq. (47), we only need the averaged potential correction

$$\int d\mathbf{x}_{e_1}\int d\mathbf{x}_{e_2}\phi_e^2(x_{e_1})\phi_e^2(x_{e_2})\delta V(\mathbf{x}_{e_1},\mathbf{x}_{e_2},\mathbf{x}_{h_1},\mathbf{x}_{h_2}) .$$

Inserting (A15) and using (A3)–(A8) one can show that the contributions with $n=0$ from the sums in (A3) and (A5) cancel exactly. Keeping again only terms up to order $(x_h/R)^3$, we obtain

$$\begin{aligned}&\int d\mathbf{x}_{e_1}\int d\mathbf{x}_{e_2}\phi_e^2(x_{e_1})\phi_e^2(x_{e_2})\delta V(\mathbf{x}_{e_1},\mathbf{x}_{e_2},\mathbf{x}_{h_1},\mathbf{x}_{h_2})\\&\quad\simeq\frac{e^2}{2R}\alpha_1[(x_{h_1}/R)^2+(x_{h_2}/R)^2]+2\Delta E ,\end{aligned} \tag{A15}$$

where ΔE is given in (A10).

[1] M. Shinada and S. Sugano, J. Phys. Soc. Jpn. **21**, 1936 (1966).

[2] For a review see, e.g., D. S. Chemla and D. A. B. Miller, J. Opt. Soc. Am. B **2**, 1155 (1985).

[3] See, e.g., the articles in *Optical Nonlinearities and Instabilities in Semiconductors,* edited by H. Haug (Academic, New York, 1988).

[4] Al. L. Efros and A. L. Efros, Fiz. Tekh. Poluprovodn. **16**, 1209 (1981) [Sov. Phys.—Semicond. **16**, 772 (1982)]; A. I. Ekimov, A. L. Efros, and A. A. Onushchenko, Solid State Commun. **56**, 921 (1985).

[5] L. E. Brus, J. Chem. Phys. **80**, 4403 (1984); IEEE J. Quantum Electron. **QE-22**, 1909 (1986), and the references to the author's earlier work.

[6] R. K. Jain and R. C. Lind, J. Opt. Soc. Am. **73**, 647 (1983).

[7] S. S. Yao, C. Karaguleff, A. Gabel, R. Fortenbery, C. T. Seaton, and G. Stegeman, Appl. Phys. Lett. **46**, 801 (1985).

[8] P. Roussignol, D. Ricard, K. C. Rustagi, and C. Flytzanis, Opt. Commun. **55**, 1431 (1985).

[9] M. C. Nuss, W. Zinth, and W. Kaiser, Appl. Phys. Lett. **49**, 1717 (1987).

[10] G. R. Olbright, N. Peyghambarian, S. W. Koch, and L. Banyai, Opt. Lett. **12**, 413 (1987).

[11] N. F. Borrelli, D. W. Hall, H. J. Holland, and D. W. Smith, J. Appl. Phys. **61**, 5399 (1987).

[12] N. Peyghambarian and S. W. Koch, Rev. Phys. Appl. **22**, 1711 (1987).

[13]M. A. Reed, R. T. Bate, K. Bradshaw, W. M. Duncan, W. R. Frensley, J. W. Lee, and H. D. Shih, J. Vac. Sci. Technol. **4**, 358 (1986).
[14]K. Kash, A. Scherer, J. M. Worlock, H. G. Craighead, and M. C. Tamargo, Appl. Phys. Lett. **49**, 1043 (1986).
[15]J. Cibert, P. M. Petroff, G. J. Dolan, S. J. Pearton, A. C. Gossard, and J. H. English, Appl. Phys. Lett. **49**, 1275 (1986).
[16]I. M. Lifshitz and V. V. Slyozov, J. Phys. Chem. Solids **19**, 35 (1961).
[17]L. Banyai and S. W. Koch, Phys. Rev. Lett. **57**, 2722 (1986).
[18]E. Hanamura, Solid State Commun. **62**, 465 (1987).
[19]D. S. Chemla and D. A. B. Miller, Opt. Lett. **11**, 522 (1986); S. Schmitt-Rink, D. A. B. Miller, and D. S. Chemla, Phys. Rev. B **35**, 8113 (1987).
[20]L. Banyai, M. Lindberg, and S. W. Koch, Opt. Lett. **13**, 212 (1988).
[21]E. Hanamura and H. Haug, Phys. Rep. **33**, 209 (1977).
[22]B. Hönerlage, R. Levy, J. B. Grun, C. Klingshirn, and K. Bohnert, Phys. Rep. **124**, 161 (1985).
[23]See, e.g., L. Allen and J. H. Eberly, *Optical Resonance and Two-Level Atoms* (Wiley, New York, 1975).